Received December 22, 2016, accepted January 3, 2017, date of publication January 5, 2017, date of current version March 2, 2017.

Digital Object Identifier 10.1109/ACCESS.2017.2648845

Underwater Image Super-Resolution by Descattering and Fusion

HUIMIN LU[1], (Member, IEEE), YUJIE LI[2], SHOTA NAKASHIMA[3], (Member, IEEE), HYONGSEOP KIM[1], (Member, IEEE), AND SEIICHI SERIKAWA[1]

[1]Kyushu Institute of Technology, Kitakyushu 8048550, Japan
[2]Yangzhou University, Yangzhou 225127, China
[3]Yamaguchi University, Ube 7538511, Japan

Corresponding author: Y. Li (yzyjli@gmail.com)

This work was supported in part by JSPS KAKENHI under Grant 15F15077, in part by the Leading Initiative for Excellent Young Researcher (LEADER) of Ministry of Education, Culture, Sports, Science and Technology-Japan, under Grant 16809746, in part by the Research Fund of Chinese Academy of Sciences under Grant MGE2015KG02, in part by the Research Fund of State Key Laboratory of Marine Geology, Tongji University, under Grant MGK1608, and in part by the Research Fund of State Key Laboratory of Ocean Engineering, Shanghai Jiaotong University, under Grant 1315 and Grant 1510.

ABSTRACT Underwater images are degraded due to scatters and absorption, resulting in low contrast and color distortion. In this paper, a novel self-similarity-based method for descattering and super resolution (SR) of underwater images is proposed. The traditional approach of preprocessing the image using a descattering algorithm, followed by application of an SR method, has the limitation that most of the high-frequency information is lost during descattering. Consequently, we propose a novel high turbidity underwater image SR algorithm. We first obtain a high resolution (HR) image of scattered and descattered images by using a self-similarity-based SR algorithm. Next, we apply a convex fusion rule for recovering the final HR image. The super-resolved images have a reasonable noise level after descattering and demonstrate visually more pleasing results than conventional approaches. Furthermore, numerical metrics demonstrate that the proposed algorithm shows a consistent improvement and that edges are significantly enhanced.

INDEX TERMS Underwater imaging, descattering, super resolution, image fusion.

I. INTRODUCTION

Currently, underwater robots, such as autonomous underwater vehicles (AUVs) and remotely operated vehicles (ROVs), are commonly used for underwater object recognition. For short-range object recognition, vision sensors are typically used to acquire high-quality images. In underwater observation, floating particles in high turbid water cause scattering. Therefore, captured underwater images suffer from poor visibility. In addition, high resolution (HR) images are desirable in ocean engineering applications such as biological and sediment analysis [1]. Although 4K imaging systems were first used in the past year, most recently installed vision sensors have low resolution (LR) and thus do not satisfy the requirements of future underwater observation [43].

Optical underwater imaging technologies, such as laser imaging, high-quality cameras, and combined modalities, have become available. Most of the imaging devices limit the image's quality. Meanwhile, it is difficult to obtain visible pleasing images at long or short distances owing to the absorptive and scattering nature of seawater. Furthermore, noise reduces the details that could contain important information. Thus, super-resolving underwater scattered images is essential for ocean observation.

Image interpolation is typically used to increase the resolution of a low resolution image. However, noisy and scattered images are processed inefficiently during interpolation. Moreover, interpolation can introduce blurring and aliasing artifacts, and it also cannot reconstruct the original edges of a scene. In the last two decades, super-resolution (SR) has been studied for enhancing the resolution of an image rapidly. SR methods can be categorized into two principal categories by inputs: multi-input [2]–[5] and single input [6]–[15].

In the multiple image SR method, an HR image is got by utilizing information from a large amount of subpixel-shifted LR images of the same scene. The key step in this method is to estimate the motion of the inputs correctly. However, the main drawback of this method is that it is difficult to estimate focus motions among multiple LR images accurately. Another issue for underwater imaging is that when the sediments are floating, it is hardly to capture the same scene in different frames at the same time. Thus, a multiple input SR method is hardly applicable in practice.

The other method is single image SR, which is named as the example-learning-based method. The merit of this method is that it does not require a series of LR images or as much motion estimation. In this method, each patch of an LR image is compared to LR database in order to extract the most similar LR patches. Depending on the training database, the single-input SR method can be further divided into two categories: external database-based [6]–[8], [14], [16] and internal database-based [9], [12], [15], [17], [18].

One of the issues for external databases is that it is difficult to set the amount and type of training images. Large-scale training datasets are usually needed to learn a sufficiently expressive LR and HR dictionary. Unfortunately, there are few underwater image databases, and there is no difference in resolution between underwater HR and LR image patch pairs.

Glasner *et al.* [19] indicated that after converting a natural image to gray scale, over 90% of the patches of an image have nine or more similar patches at the same scale. Moreover, more than nine patches have the same similarity at different scales. Hence, the recurrence of patches across scales provides the basis for applying example-based SR.

Scatter and noise corruption are ubiquitous phenomena in underwater imaging affecting image processing tasks. The conventional approaches [19] have previously been used for denoising using non-local means (NLM) [20] or block-matching and three-dimensional (3D) filtering (BM3D) [21] and a regularization prior for inverse problems [22]. Potter *et al.* [23] proposed a SR method for gaining higher-resolution video frames using the SR constraints to similar patches. However, with regard to Singh *et al.*'s work [12], although both denoising and super resolving involve the same patch-based priors, they are utilized toward different objectives. Denoising is intended to smoothen similar patches to remove noise in the patch. The goal of SR is to seek more similar patches at different scales to enhance the textural content of each patch. Hence, Singh *et al.* [12] proposed the fusion method to eliminate the signal loss caused by denoising using SR and denoising simultaneously. However, both Singh et al.'s work and sparse-coding-based super resolving methods can deal with low levels of noise. These methods cannot solve the heavy noisy images.

Building on some initial work [24], we propose further development in a novel framework for scattered-image SR. Our algorithm begins with initial descattering and color correction. The first descattered image is obtained in accordance with [24]. After large amounts of scatter are removed, the resulting image contains a low level of scatter and substantial noise. Thus, a fast denoising and descattering algorithm is proposed. We call this result the preprocessed LR image. After this, we super-resolve the descattered and preprocessed LR images using an example-based SR algorithm, resulting in descattered and preprocessed SR images, respectively. Finally, we obtain the noise-free SR image by fusing the visual information in two images.

In this paper, we have contributed the following items. First, we can super-resolve a highly turbid underwater image using the proposed framework. This overcomes limitations in the conventional SR methods. Second, the proposed method can obtain a visually pleasing result with better textures. Third, unlike the conventional SR methods in natural scenes, the SR method we propose takes light compensation into consideration. Abundant experimental results show that our method achieves excellent SR results and also removes artifacts and scattering effectively.

II. RELATED WORK

This paper concerns super-resolving underwater images and descattering. To the best of our knowledge, there are few SR reconstruction algorithms for underwater imaging. Zhu *et al.* [38] proposed a preprocessing step for removing noise and simply applied SR to images. This method does not consider scatter effects, light absorption, or texture loss. Thus, we propose a novel scheme for underwater SR and descattering simultaneously in this article. In the next section, we introduce the recent trends of descattering and super-resolution methods.

A. DESCATTERING

Descattering and SR are two principal methods in this paper. Let us recall most of the recent methods regarding these technologies. In reviewing recent studies, research related to image descattering or dehazing can be classified into the following two principal groups.

1) MULTI-LIGHTING

Narasimham *et al.* [25]–[27] and Tsiotsios *et al.* [28] proposed the useage of multiple lights to estimate the backscatter from a scene. Treibitz and Schechner [29] proposed fusing images obtained using two-directional illumination to create a single clearer image. However, it is difficult to recover the time variations adverse to visibility in the presence of floating turbidity sediments.

2) PRIOR

Fattal [30] proposed to use principal component analysis (PCA) for descattering. He *et al.* [31] analyzed a large amount of natural sky images and concluded that there is a dark channel in most of color images. They accordingly proposed a dark channel prior algorithm. However, these methods resulted in regional contrast shading that could cause halos or aliasing.

B. SUPER RESOLUTION

The principal idea of image super resolution is to reconstruct an HR image using interpolation and reconstruction of LR image patches, learning, and indexing for the best matching patches as the HR map. In this paper, we focus on a single-image SR method. As mentioned in the introduction, according to the source of training data, single-image SR can be summarized to 3 principal categories.

1) EXTERNAL DATABASE-DRIVEN SR

These kind of methods use learning algorithms to study the LR-HR mapping from an existing LR-HR database. There are many learning algorithms for super-resolving LR images, such as nearest neighbor [6], kernel ridge regression [32], sparse coding [8], manifold learning [33], and CNNs [14]. The principal challenge is how to model the patch space effectively. Instead of studying a global mapping over the entire database, some models attempt to reduce computational complexity by partitioning or pre-clustering the external database [15], [34]. Other approaches such as dimensionality reduction [16], [35] and higher-level features extraction [36] are also used for learning LR-HR mapping.

2) INTERNAL DATABASE-DRIVEN SR

Glasner *et al.* [19] proposed a self-similar patch-based SR algorithm using a natural statics model. Freeman and Fattal [18] determined further that self-similar patches is existed in spatial neighbor patches. Gao *et al.* [9] first introduced sparse neighbor embedding for searching self-similar patches. Singh *et al.* [12] used the self-similarity ideas for solving noisy image SR.

3) UNIFIED DATABASE-DRIVEN SR

Singh and Ahuja [37] proposed a sub-band texture patterns similarity-based method for SR. Zhu *et al.* [38] used optical flow-based patch deformation as a dictionary searching rule. Huang *et al.* [13] proposed a transformed self-exemplars method for single-image SR. Textures can be recovered well through the use of geometric variation.

III. SR USING DESCATTERING AND FUSION

Considering that scattering and noise are included in underwater imaging, the observation model is

$$Y_\lambda(x) = DLI_\lambda(x) + n, \lambda \in \{r, g, b\} \quad (1)$$

where $Y_\lambda(x)$ is the LR underwater image, $I_\lambda(x)$ is the HR underwater image, the matrices D and L represent downsampling and blurring, respectively, and n is the noise generated. The SR reconstruction problem is to estimate the underlying HR image $I_\lambda(x)$ of $Y_\lambda(x)$. We assume the noise to be independent and identically distributed (I.I.D.), with variance σ^2. Considering that the HR image $I_\lambda(x)$ contains scatters, (1) can be written as

$$Y_\lambda(x) = DL\,(J_\lambda(x)t_\lambda(x) + (1 - t_\lambda(x))A_\lambda) + n,\ \lambda \in \{r, g, b\} \quad (2)$$

where $J_\lambda(x)$ is the clean image, $t_\lambda(x)$ is the transmission map, and A_λ is the ambient light. Assuming that the ambient light and transmission map are known, the estimated $\hat{J}_\lambda(x)$ is (3), as shown at the top of the next page.

Because $t_\lambda(x) \in [0,\ 1]$, (3) implies that except when haze is absent ($t_\lambda(x) = 1$), the noise contribution is amplified. Hence, in this paper, we propose a new framework for recovering the HR turbidity of underwater images.

As shown in Figure 1, we first consider performing simultaneous underwater descattering and denoising (SUDD) to remove the scattering and noise. Next, we super-resolve the preprocessed and further denoised images using the SR algorithm. We propose an image fusion method for combining the texture, spatial, frequency, luminance, and chrominance components. Our proposed framework preserves richer edge information than that obtained using the traditional processing method. Meanwhile, the super-resolved image has no color shifts.

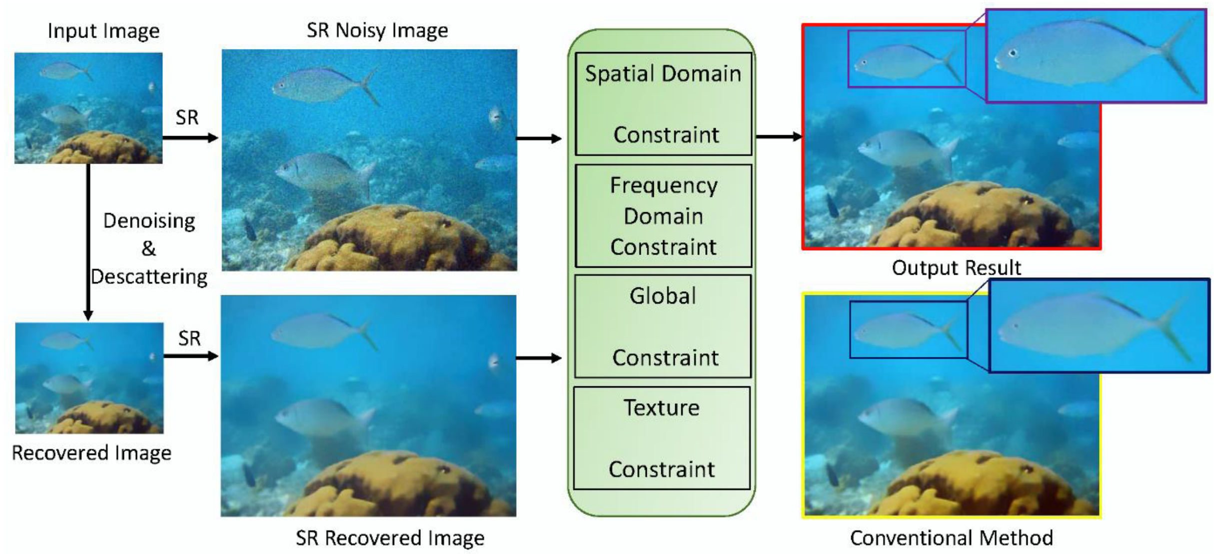

FIGURE 1. **Pipeline of proposed approach for obtaining a noise-free HR image from a turbid LR image.**

$$\hat{J}_\lambda(x) = \frac{Y_\lambda(x) - DL\left((1-t_\lambda(x))A_\lambda\right)}{DLt_\lambda(x)}$$
$$= \frac{DL\left(J_\lambda(x)t_\lambda(x)\right) + DL\left((1-t_\lambda(x))A_\lambda\right) + n - DL\left((1-t_\lambda(x))A_\lambda\right)}{DLt_\lambda(x)}$$
$$= J_\lambda(x) + \frac{n}{DLt_\lambda(x)}, \quad \lambda \in \{r, g, b\} \tag{3}$$

A. SIMULTANEOUS DESCATTERING AND DENOISING

Most descattering algorithms can remove heavy haze perfectly, but because they use local patches for estimating the transmission, the algorithms cause additional noise in the final descattered result. In this paper, we propose the noisy-scatter model

$$Y^s_\lambda(x) = I_\lambda(x)t_\lambda(x) + B_\lambda(x) + n \tag{4}$$

where $B_\lambda(x) = (1 - t_\lambda(x))A_\lambda(x)$. Following the non-parametric kernel regression [39], we can write the estimation problem of each color channel as

$$\min_{I_\lambda, B_\lambda} \sum_{x_i \in \Omega(x)} \left[Y^s_\lambda(x_i) - I_\lambda(x_i)t_\lambda(x_i) - B_\lambda(x_i)\right]^2 K_{H_i}(x_i - x) \tag{5}$$

where $\Omega(x)$ is a neighborhood around the pixel x, and K_{H_i} is the locally adaptive regression kernel. We estimate the ambient light $A_\lambda(x)$ according to the color lines. As described in [39] and [40], the orientation of the atmospheric light vector is calculated by utilizing the abundant small image patches in the image.

Since Eq. (5) is a minimization operation with two unknowns, our purpose is to find the solution iteratively. We solve it as two separate minimization problems, and alternate between them for solving $I_\lambda(x_i)$ and $B_\lambda(x_i)$. We further assume a 0-th order regression model

$$\min_{I_\lambda} \sum_{x_i \in \Omega(x)} \left[Y'^s_\lambda(x_i) - I_\lambda(x_i)t_\lambda(x_i)\right]^2 K_{H_i}(x_i - x) \tag{6}$$

$$\min_{B_\lambda} \sum_{x_i \in \Omega(x)} \left[Y''^s_\lambda(x_i) - P_\lambda(x_i)B_\lambda(x_i)\right]^2 K_{H_i}(x_i - x) \tag{7}$$

where $Y'^s_\lambda(x_i) = Y^s_\lambda(x_i) - B_\lambda(x_i)$, $Y''^s_\lambda(x_i) = Y^s_\lambda(x_i) - I_\lambda(x_i)$, and $P_\lambda(x_i) = 1 - \frac{1}{A_\lambda(x_i)} I_\lambda(x_i)$. Then, we can use the weighted least-squares solution are

$$\hat{I}_\lambda(x) = \frac{\sum_{x_i \in \Omega(x)} K_{H_i}(x_i - x)t_\lambda(x_i)Y'^s_\lambda(x_i)}{\sum_{x_i \in \Omega(x)} K_{H_i}(x_i - x)t_\lambda(x_i)^2} \tag{8}$$

$$\hat{B}_\lambda(x) = \frac{\sum_{x_i \in \Omega(x)} K_{H_i}(x_i - x)P_\lambda(x_i)Y''^s_\lambda(x_i)}{\sum_{x_i \in \Omega(x)} K_{H_i}(x_i - x)P_\lambda(x_i)^2} \tag{9}$$

Although the filtering is linear, the steering kernels are computed on the received data and the result is a non-liner filter. In this algorithm, we utilize Mean Square Error (MSE) of scene radiance to stop the regression.

The full scatter and noise removal procedure are summarized in Algorithm 1.

Algorithm 1 Simultaneous Descattering and Denoising

1. Initial
 Estimate $\hat{I}$ by using NLM to denoise input image Y^s_λ
 Estimate transmission t_λ and ambient light A_λ from $\hat{I}$ using color lines [41]
 Descatter $\hat{I}$ through an underwater dark channel prior [24]
2. Second round estimation of I_λ
3. Iterate between the estimates for $\hat{I}_\lambda$ and $\hat{B}_\lambda$ until the minimum mean square error (MSE) is reached
While $MSE \geq MSE_{\min}$ do
  Estimate $\hat{I}_\lambda$ using $\hat{B}_\lambda$ (Eq. 6)
  Estimate $\hat{B}_\lambda$ using $\hat{I}_\lambda$ (Eq. 7)
 end while

B. SR

High-resolution cameras tend to be used for high resolution of underwater images. However, most recent AUVs or ROVs are equipped with low-resolution cameras. Using a SR method is one of the most effective approaches for resolving this issue. As a result of the complexity of underwater environments, such as heavy scatters and low contrast, it is difficult to use external database-driven SR methods. Consequently, the proposed algorithm has the advantage of requiring neither external training databases nor fully self-internal SR algorithms [13].

After that, let us consider the estimate $\hat{I}^{new}_\lambda$ of recovered image $\hat{I}_\lambda$ that is obtained by taking a convex combination of denoised image $\hat{I}^{dn}_\lambda$ and noisy image $\hat{I}^n_\lambda$

$$\hat{I}^{new}_\lambda = (1 - R) \cdot \hat{I}^{dn}_\lambda + R \cdot \hat{I}^n_\lambda \tag{10}$$

where '$\bullet$' is the Hadamard product, and the weighting matrix R contains values in [0, 1].

We transfer Eq. (10) into the frequency domain as

$$\hat{F}^{new(r,s)}_\lambda = (1 - \mathbf{R}^{(r,s)}) * \hat{F}^{dn(r,s)}_\lambda + \mathbf{R}^{(r,s)} * \hat{F}^{n(r,s)}_\lambda \tag{11}$$

where r and s denote its scale and orientation bands per scale, respectively. We further re-parameterize $\mathbf{R}^{(r,s)}$ to the form

$$\mathbf{R}^{(r,s)} = \alpha T \cdot V \cdot W^{(r,s)} \tag{12}$$

where α is the scalar parameter ($0 < \alpha < 1$). It globally controls the relative weights of the overly smooth $\hat{I}^{dn}_\lambda$ and

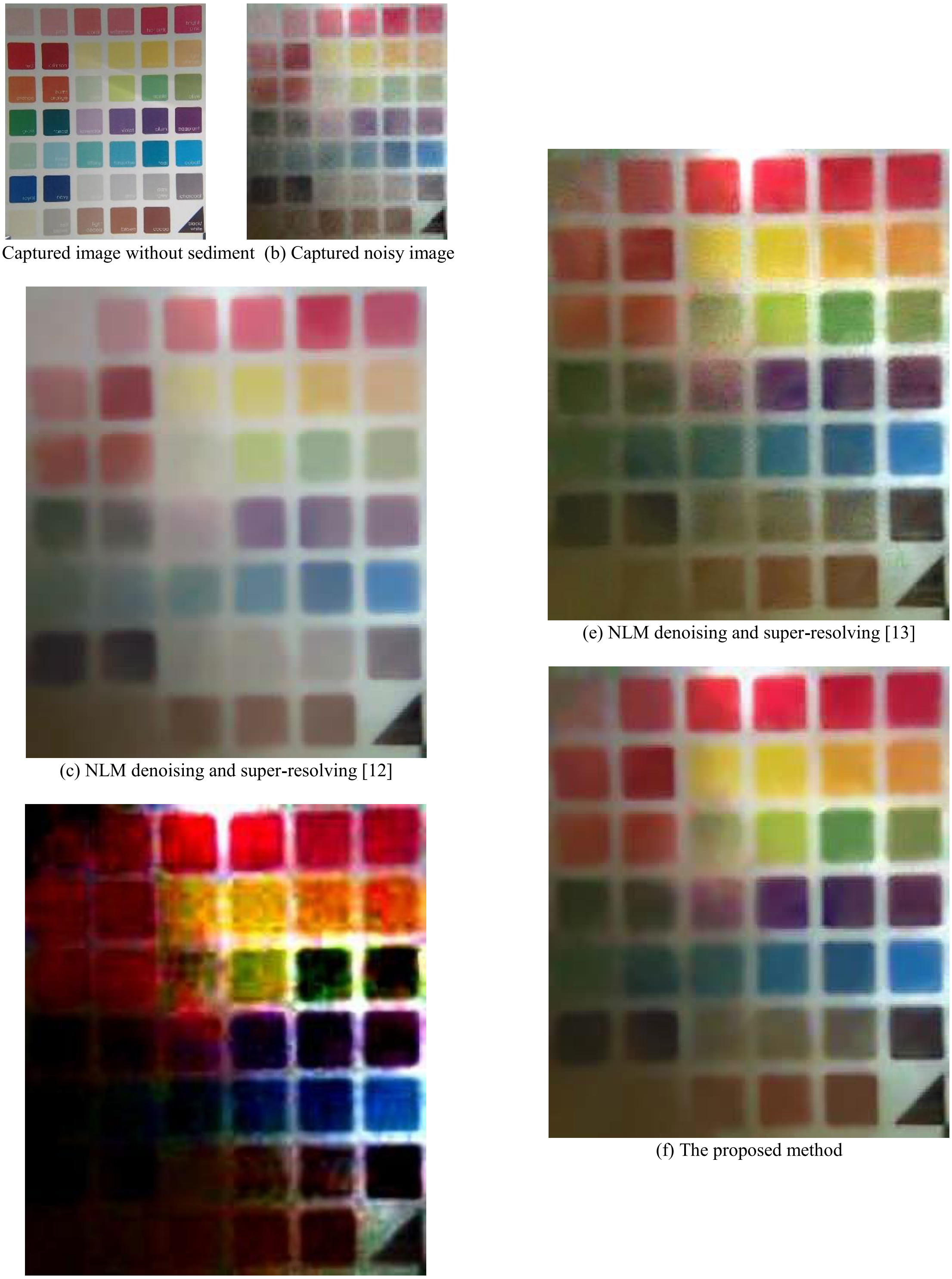

(a) Captured image without sediment (b) Captured noisy image

(c) NLM denoising and super-resolving [12]

(d) Descattering [31] and super-resolving [9]

(e) NLM denoising and super-resolving [13]

(f) The proposed method

FIGURE 2. Simulation results of water tank. (a) Captured image without sediments and noise. (b) Captured image with 200 mg/L turbidity and additional noise. (c) Super-resolved result using the method in [12]. (d) Super-resolved result using the method in [9]. (e) Super-resolved result using the method in [13]. (f) Super-resolved result using the proposed method. (a) Captured image without sediment (b) Captured noisy image. (c) NLM denoising and super-resolving [12]. (d) Descattering [31] and super-resolving [9]. (e) NLM denoising and super-resolving [13]. (f) The proposed method.

the noisy $\hat{I}^n_\lambda$ in the result. T is the value that evaluates the target patch to its best matching source patch when super-resolving [13]. $W^{(r,s)}$ is the frequency constraint that facilitates selective blending of the frequency and orientation band [12]. V is the variance map that measures the ''texture-less'' of the local patches [12].

(a) Captured image without sediment

(b) Captured noisy image

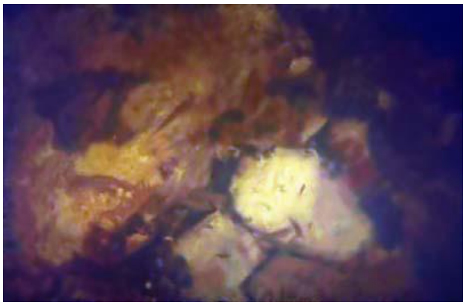

(c) NLM denoising and super-resolving [12]

(d) Descattering [31] and super-resolving [9]

(e) NLM denoising and super-resolving [13]

(f) Proposed method

FIGURE 3. Underwater objects. (a) Captured image without sediments and noise. (b) Captured image with turbidity and additional noise. (c) Super-resolved result using the method in [12]. (d) Super-resolved result using the method in [9]. (e) Super-resolved result using the method in [13]. (f) Super-resolved result using the proposed method. (a) Captured image without sediment (b). Captured noisy image. (c) NLM denoising and super-resolving [12]. (d) Descattering [31] and super-resolving [9]. (e) NLM denoising and super-resolving [13]. (f) Proposed method.

IV. EXPERIMENTAL RESULTS

A. IMAGE QUALITY METRICS

We also use some quality assessment rules to compare the results of different methods. This analysis includes the peak signal to noise ratio (PSNR) [42], structural similarity (SSIM) [42], and color distance [43]. Here, we propose a new quality assessment rule for underwater images. First, we recall some conventional image quality indices.

Metric ΔE represents the Euclidean distance between two colors in the *Lab* color space. It is calculated from their L, a, and b values as follows:

$$\Delta E(A, B) = \sqrt{(L_A - L_B)^2 + (a_A - a_B)^2 + (b_A - b_B)^2} \tag{13}$$

where smaller ΔE values indicate greater similarity between images A and B. Table 1 shows that the SSIM and ΔE values of the proposed method is superior than the others.

B. WATER TANK SIMULATION

Twenty underwater images were selected, including five images from the Internet, five images from JAMSTEC JDI Datasets, and ten images from our water tank experiments. In the water tank experiments, an underwater camera (OLYMPUS μTough TG2) was placed in the water. The objects were placed at a depth of 30 cm. The distance between the objects and the camera was approximately 60 cm. We used Intel Core i7 CPU, 4G RAM computer for computing. The size of input image was 400×470 pixels. The performance of the proposed algorithm is evaluated both analytically and experimentally using ground truths. We also compare the proposed method with other currently proposed state-of-the-art methods. The results demonstrate that the proposed method shows superior scatter/noise removal without ring artifacts. The computational time of this image is about 10 seconds. Figure 2 shows the experimental results in detail.

Figure 2 shows the simulation results in the water tank. We added deep-sea soil to the clean ocean water at a turbidity of 200 mg/L, and we also added additional noise to the captured image ($\sigma = 10$). Figure 2(c) presents the super-resolved image using Singh et al.'s method [12]. In that method, noise and edge information were fully considered. However, the resulting image retains some haze. The most recent dehazing method [31] and the SR method [9] were used to remove the scatter as well as to enlarge the image. However, as a result of non-ideal dehazing, the final result contains non-uniform haze and additional artifacts. While Huang et al.'s method [13] considered the use of transferred self-examples in super-resolving, the remaining heavy noise leads to an uncomfortable result with ring artifacts. Compared with the other methods, the proposed method performs better in preserving color and super-resolving. Table 1 shows the numerical metrics of different methods. Although PSNR value of the proposed method is lower than NLM+SR method, but the SSIM and ΔE is better than the others.

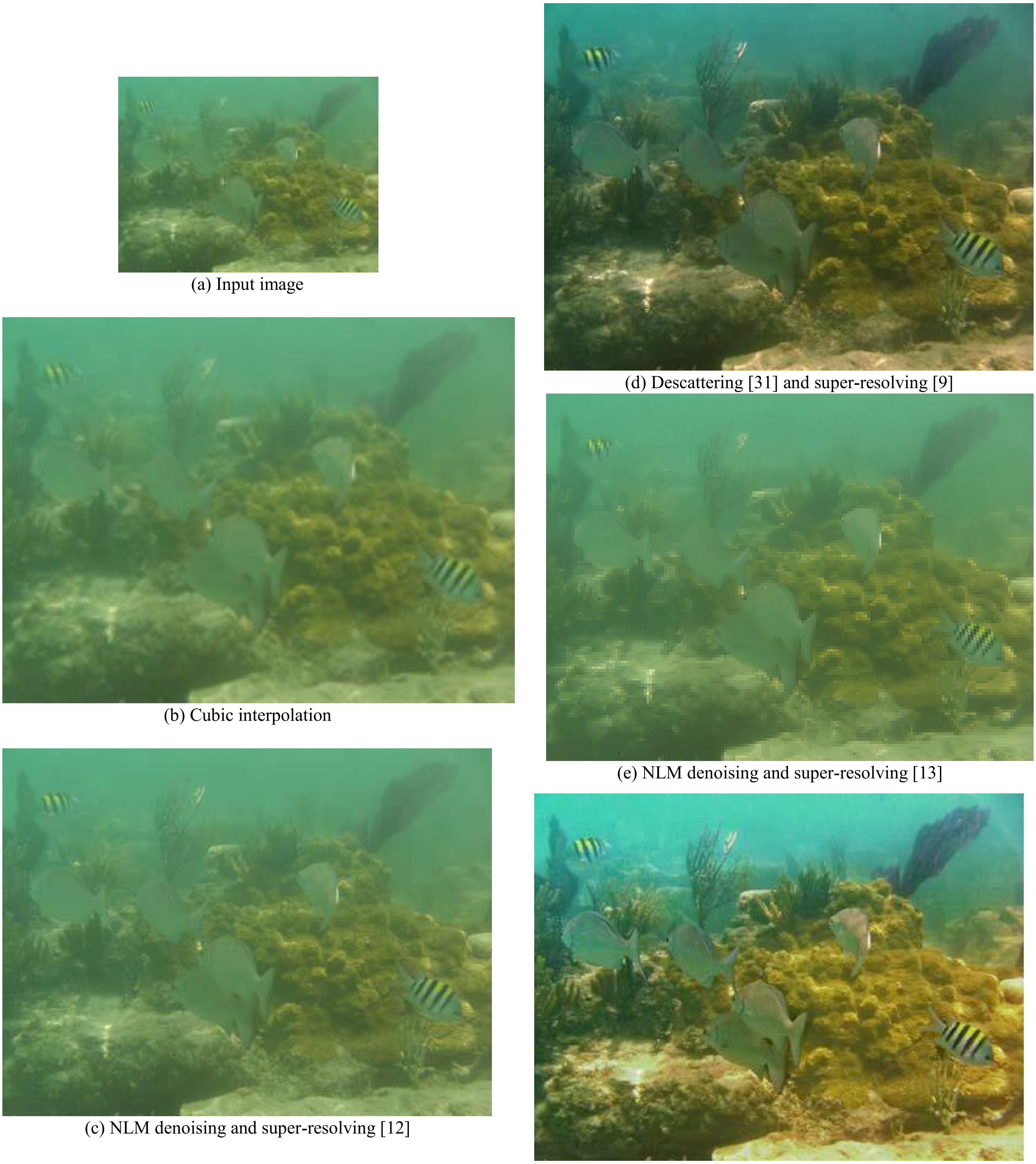

(a) Input image

(b) Cubic interpolation

(c) NLM denoising and super-resolving [12]

(d) Descattering [31] and super-resolving [9]

(e) NLM denoising and super-resolving [13]

(f) Proposed method

FIGURE 4. Underwater objects. (a) Captured image. (b) Cubic interpolation result. (c) Super-resolved result using the method in [12]. (d) Super-resolved result using the method in [9]. (e) Super-resolved result using the method in [13]. (f) Super-resolved result using the proposed method. (a) Input image. (b) Cubic interpolation. (c) NLM denoising and super-resolving [12]. (d) Descattering [31] and super-resolving [9]. (e) NLM denoising and super-resolving [13]. (f) Proposed method.

C. REAL-WORLD EXPERIMENT

In the second experiment, we take underwater images from the Internet [44]. Figure 3 indicates the experimental results of a real-world scene that was captured in turbid water. The size of the image is 350×227 pixels. The super-resolved image is 700×454 pixels ($2\times$). From Figure 3, we can

TABLE 1. Comparison of the different methods in Figure 2

Method	PSNR	SSIM	ΔE
NLM + SR [12]	**14.7197**	0.6716	35.3922
DCP [31] + SR [9]	8.0379	0.2937	87.7031
NLM + SR [13]	14.1968	0.6720	30.1589
Proposed	14.6315	**0.6831**	**29.1759**

TABLE 2. Comparison Results of Different Methods in Figure 3

Method	PSNR	SSIM	ΔE
NLM + SR [12]	21.4148	0.7329	21.9372
DCP [31] + SR [9]	14.0884	0.5639	55.8729
NLM + SR [13]	17.9248	0.7389	26.0950
Proposed	**21.4726**	**0.8231**	**17.7678**

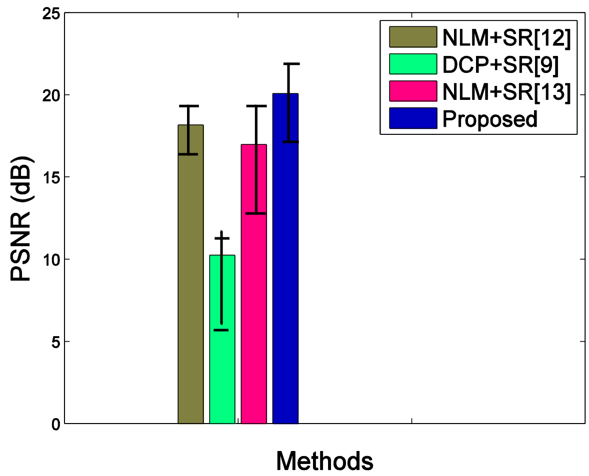

FIGURE 5. Mean PSNR (dB) results of the different methods.

also conclude that the proposed method outperforms the other state-of-the-art methods.

Table 2 shows the quantitative analysis results. The results show that the proposed method outperform the other methods. The images were offered at https://sites.google.com/site/kyutech8luhuimin. Figure 4 shows the other experiment of real-world underwater images super resolution by different methods. We can conclude that the proposed method can achieve a visual pleasing result.

D. PERFORMANCE EVALUATION

To complement the discussions in the previous sections, we provide experimental evaluations for representative techniques by 200 images. The evaluation for image SR and descattering can be measured by PSNR, SSIM etc. Figure 5 shows the mean PSNR (dB) results of these methods. Figure 6 shows the mean SSIM values of these methods. In summary, the proposed method has the highest mean PSNR and mean SSIM values.

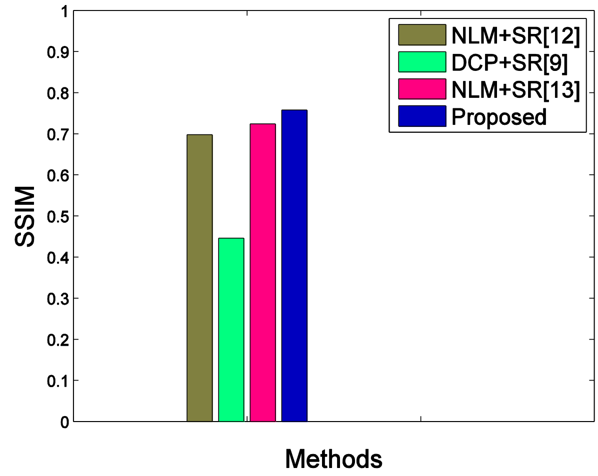

FIGURE 6. Mean SSIM results of the different methods.

V. CONCLUSIONS

In this paper, we presented SR method for recovering distorted images in high turbid water. We have overcome the noise or artifacts in high resolved scattered images. The HR image of scattered and descattered images is obtained using a self-similarity SR algorithm. Then, a proposed convex fusion rule is applied to recover the final HR image. The super-resolved images have a reasonable noise level after descattering and demonstrate visually more pleasing results than images obtained using conventional approaches. Furthermore, numerical metrics demonstrated that the proposed algorithm shows consistent image improvement, with significant improvement for the edges. In future, we will focus on solving the inhomogeneous scatters and artificial lighting issues in SR. Furthermore, the cloud computing [45]–[48] should be applied in the proposed SR system.

REFERENCES

[1] D. M. Kocak, F. R. Dalgleish, F. M. Caimi, and Y. Y. Schechner, "A focus on recent developments and trends in underwater imaging," *Marine Technol. Soc. J.*, vol. 42, no. 1, pp. 52–67, 2008.

[2] T. Huang and R. Tsai, "Multi-frame image restoration and registration," *Adv. Comput. Vis. Image Process.*, vol. 1, no. 2, pp. 317–339, 1984.

[3] M. Irani and S. Peleg, "Improving resolution by image registration," *Graph. Models Image Process.*, vol. 53, no. 3, pp. 231–239, May 1991.

[4] M. Irani and S. Peleg, "Motion analysis for image enhancement: Resolution, occlusion, and transparency," *J. Vis. Commun. Image Represent.*, vol. 4, no. 4, pp. 324–335, Dec. 1993.

[5] S. Farsiu, M. D. Robinson, M. Elad, and P. Milanfar, "Fast and robust multiframe super resolution," *IEEE Trans. Image Process.*, vol. 13, no. 10, pp. 1327–1344, Oct. 2004.

[6] W. T. Freeman, T. R. Jones, and E. C. Pasztor, "Example-based super-resolution," *IEEE Comput. Graph. Appl.*, vol. 22, no. 2, pp. 56–65, Mar./Apr. 2002.

[7] K. I. Kim and Y. Kwon, "Example-based learning for single-image super-resolution," in *Proc. DAGM*, Jun. 2008, pp. 456–465.

[8] J. Yang, J. Wright, T. Huang, and Y. Ma, "Image super-resolution as sparse representation of raw image patches," *IEEE Trans. Image Process.*, vol. 19, no. 11, pp. 2861–2873, Nov. 2010.

[9] X. Gao, K. Zhang, D. Tao, and X. Li, "Single-image super-resolution with sparse neighbor embedding," *IEEE Trans. Image Process.*, vol. 21, no. 7, pp. 3194–3205, Jul. 2012.

[10] K. S. Ni and T. Q. Nguyen, "Image superresolution using support vector regression," *IEEE Trans. Image Process.*, vol. 16, no. 6, pp. 1596–1610, Jun. 2007.
[11] D.-H. Trinh, M. Luong, F. Dibos, J.-M. Rocchisani, C.-D. Pham, and T. Q. Nguyen, "Novel example-based method for super-resolution and denoising of medical images," *IEEE Trans. Image Process.*, vol. 23, no. 4, pp. 1882–1895, Apr. 2014.
[12] A. Singh, F. Porikli, and N. Ahuja, "Super-resolving noisy images," in *Proc. CVPR*, Jun. 2014, pp. 2846–2853.
[13] J.-B. Huang, A. Singh, and N. Ahuja, "Single image super-resolution from transformed self-exemplars," in *Proc. CVPR*, Jun. 2015, pp. 5197–5206.
[14] C. Dong, C. C. Loy, K. He, and X. Tang, "Learning a deep convolutional network for image super-resolution," in *Proc. ECC*, Sep. 2014, pp. 184–199.
[15] R. Timofte, V. De Smet, and L. V. Gool, "A+: Adjusted anchored neighborhood regression for fast super-resolution," in *Proc. ACC*, Nov. 2014, pp. 1–16.
[16] J. Sun, J. Sun, Z. Xu, and H.-Y. Shum, "Gradient profile prior and its applications in image super-resolution and enhancement," *IEEE Trans. Image Process.*, vol. 20, no. 6, pp. 1529–1542, Jun. 2011.
[17] J. Yang, Z. Lin, and S. Cohen, "Fast image super-resolution based on in-place example regression," in *Proc. CVPR*, Jun. 2013, pp. 1059–1066.
[18] G. Freedman and R. Fattal, "Image and video upscaling from local self-examples," *ACM Trans. Graph.*, vol. 30, no. 2, Apr. 2011, Art. no. 12.
[19] D. Glasner, S. Bagon, and M. Irani, "Super-resolution from a single image," in *Proc. ICC*, Sep. 2009, pp. 349–356.
[20] A. Buades, B. Coll, and J.-M. Morel, "A non-local algorithm for image denoising," in *Proc. IEEE Comput. Soc. Conf. Comput. Vis. Pattern Recognit.*, vol. 2. San Diego, CA, USA, Jun. 2005, pp. 60–65.
[21] K. Dabov, A. Foi, V. Katkovnik, and K. Egiazarian, "Image denoising by sparse 3-D transform-domain collaborative filtering," *IEEE Trans. Image Process.*, vol. 16, no. 8, pp. 2080–2095, Aug. 2007.
[22] G. Peyré, S. Bougleux, and L. Cohen, "Non-local regularization of inverse problems," in *Proc. ECC*, Oct. 2008, pp. 57–68.
[23] M. Protter, M. Elad, H. Takeda, and P. Milanfar, "Generalizing the nonlocal-means to super-resolution reconstruction," *IEEE Trans. Image Process.*, vol. 18, no. 1, pp. 36–51, Jan. 2009.
[24] H. Lu, Y. Li, L. Zhang, and S. Serikawa, "Contrast enhancement for images in turbid water," *J. Soc. Amer. A*, vol. 32, no. 5, pp. 886–893, 2015.
[25] S. G. Narasimhan and S. K. Nayar, "Contrast restoration of weather degraded images," *IEEE Trans. Pattern Anal. Mach. Learn.*, vol. 25, no. 6, pp. 713–724, Jun. 2003.
[26] F. Cozman and E. Krotkov, "Depth from scattering," in *Proc. IEEE Conf. Comput. Vis. Pattern Recognit.*, Jun. 1997, pp. 801–806.
[27] S. G. Narasimhan, S. K. Nayar, B. Sun, and S. J. Koppal, "Structured light in scattering media," in *Proc. IEEE Int. Conf. Comput. Vis.*, Oct. 2005, pp. 420–427.
[28] C. Tsiotsios, M. E. Angelopoulou, T.-K. Kim, and A. J. Davison, "Backscatter compensated photometric stereo with 3 sources," in *Proc. IEEE Conf. Comput. Vis. Pattern Recognit.*, Jun. 2014, pp. 4321–4328.
[29] T. Treibitz and Y. Y. Schechner, "Turbid scene enhancement using multi-directional illumination fusion," *IEEE Trans. Image Process.*, vol. 21, no. 11, pp. 4662–4667, Nov. 2012.
[30] R. Fattal, "Single image dehazing," *ACM Trans. Graph.*, vol. 27, no. 3, Aug. 2008, Art. no. 72.
[31] K. He, J. Sun, and X. Tang, "Single image haze removal using dark channel prior," *IEEE Trans. Pattern Anal. Mach. Intell.*, vol. 33, no. 12, pp. 2341–2353, Dec. 2011.
[32] K. I. Kim and Y. Kwon, "Single-image super-resolution using sparse regression and natural image prior," *IEEE Trans. Pattern Anal. Mach. Intell.*, vol. 32, no. 6, pp. 1127–1133, Jun. 2010.
[33] H. Chang, D.-Y. Yeung, and Y. Xiong, "Super-resolution through neighbor embedding," in *Proc. IEEE Conf. Comput. Vis. Pattern Recognit. (CVPR)*, vol. 1. Jun./Jul. 2004, pp. 275–282.
[34] R. Timofte, V. De Smet, and L. Van Gool, "Anchored neighborhood regression for fast example-based super-resolution," in *Proc. ICCV*, Dec. 2013, pp. 1920–1927.
[35] R. Fattal, "Image upsampling via imposed edge statistics," *ACM Trans. Graph.*, vol. 26, no. 3, 2007, Art. no. 95.
[36] J. Sun, J. Zhu, and M. F. Tappen, "Context-constrained hallucination for image super-resolution," in *Proc. CVPR*, Jun. 2010, pp. 231–238.
[37] A. Singh and N. Ahuja, "Super-resolution using sub-band self-similarity," in *Proc. ICP*, 2014, pp. 4447–4452.
[38] Y. Zhu, Y. Zhang, and A. L. Yuille, "Single image super-resolution using deformable patches," in *Proc. CVPR*, Jun. 2014, pp. 2917–2924.
[39] H. Takeda, S. Farsiu, and P. Milanfar, "Kernel regression for image processing and reconstruction," *IEEE Trans. Image Process.*, vol. 16, no. 2, pp. 349–366, Feb. 2007.
[40] Y. Chen, W. Li, M. Xia, Q. Li, and K. Yang, "Super-resolution reconstruction for underwater imaging," *Opt. Appl.*, vol. 41, no. 4, pp. 841–853, 2011.
[41] R. Fattal, "Dehazing using color-lines," *ACM Trans. Graph.*, vol. 34, no. 1, Nov. 2014, Art. no. 13.
[42] H. Lu, L. Zhang, and S. Serikawa, "Maximum local energy: An effective approach for multisensory image fusion in beyond wavelet transform domain," *Comput. Math. Appl.*, vol. 64, no. 5, pp. 996–1003, 2012.
[43] H. Lu, Y. Li, S. Nakashima, and S. Serikawa, "Turbidity underwater image restoration using spectral properties and light compensation," *IEICE Trans. Inf. Syst.*, vol. E99-D, no. 1, pp. 219–227, 2016.
[44] F. Codevilla, J. D. O. Gaya, N. D. Filho, and S. S. C. Botelho, "Achieving turbidity robustness on underwater images local feature detection," in *Proc. BMV*, 2015, pp. 1–10.
[45] Y. Zhang, M. Chen, D. Huang, D. Wu, and Y. Li, "iDoctor: Personalized and professionalized medical recommendations based on hybrid matrix factorization," *Future Generat. Comput. Syst.*, vol. 66, pp. 30–35, Jan. 2017.
[46] Y. Zhang, "GroRec: A group-centric intelligent recommender system integrating social, mobile and big data technologies," *IEEE Trans. Services Comput.*, vol. 9, no. 5, pp. 786–795, Sep./Oct. 2016.
[47] Y. Zhang, M. Chen, S. Mao, L. Hu, and V. Leung, "CAP: Community activity prediction based on big data analysis," *IEEE Netw.*, vol. 28, no. 4, pp. 52–57, Jul. 2014.
[48] Y. Zhang, D. Zhang, M. M. Hassan, A. Alamri, and L. Peng, "CADRE: Cloud-assisted drug recommendation service for online pharmacies," *Mobile Netw. Appl.*, vol. 20, no. 3, pp. 348–355, Jun. 2014.

HUIMIN LU (M'12) received the B.S. degree in electronics information science and technology from Yangzhou University in 2008, the M.S. degrees in electrical engineering from the Kyushu Institute of Technology and Yangzhou University in 2011, and the Ph.D. degree in electrical engineering from the Kyushu Institute of Technology in 2014. From 2013 to 2016, he is a JSPS Research Fellow with the Kyushu Institute of Technology, where he is currently an Assistant Professor. His research interests include computer vision, robotics, artificial intelligence, and ocean observing.

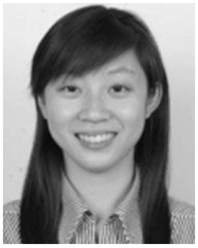

YUJIE LI received the B.S. degree in computer science and technology from Yangzhou University in 2009, the M.S. degrees in electrical engineering from the Kyushu Institute of Technology and Yangzhou University in 2012, and the Ph.D. degree from the Kyushu Institute of Technology in 2015. She is currently a Lecturer with Yangzhou University. Her research interests include computer vision, sensors, and image segmentation.

SHOTA NAKASHIMA (M'13) received the Ph.D. degree in electrical engineering from the Kyushu Institute of Technology in 2010. From 2010 to 2012, he was an Assistant Professor with the Ube National College of Technology. He is currently a Senior Assistant Professor with Yamaguchi University. His current research interests include image processing, intelligent sensing, and artificial life. He is a member of SICE and IIAE.

HYOUNGSEOP KIM (M'09) received the B.A. degree in electrical engineering and the master's and Ph.D. degrees from the Kyushu Institute of Technology in 1994, 1996, and 2001, respectively. He is currently a Professor with the Department of Control Engineering, Kyushu Institute of Technology. His research interests include medical application of image analysis.

SEIICHI SERIKAWA received the B.S. and M.S. degrees from Kumamoto University, in 1984 and 1986, respectively, and the Ph.D. degree from the Kyushu Institute of Technology in 1994, all in electronic engineering. He is currently a Vice President with the Kyushu Institute of Technology and also serves as a Professor with the Center for Socio-Robotic Synthesis and the Department of Electrical and Electronic Engineering. His current research interests include computer vision, sensors, and robotics.